Distribution Analysis of Electrode Reaction of Lithium Manganese Oxide As Studied by XAFS Imaging Technique

Hirona Yamagishi, Ryota Miyahara, Misaki Katayama, and Yasuhiro Inada

Department of Applied Chemistry, College of Life Sciences, Ritsumeikan University, 1-1-1 Noji-Higashi, Kusatu 525-8577, Japan

1. Introduction

Lithium ion secondary batteries are widely used as useful energy storage devices, and it is essential to evaluate the reaction distribution appeared in the electrode to improve their performance. The XAFS imaging technique is quite powerful to visualize the in-plane reaction distribution under the operating conditions, and it has been shown that the heterogeneous distribution is generated due to the difference in the electron conductivity for the lithium iron phosphate ($LiFePO_4$, LFP) cathode [1]. The distribution analyses for the other cathode materials with different crystal structure are necessary to understand the generation mechanism of the heterogeneous distribution. In the previous study, the 2D XAFS imaging measurements were performed for the lithium manganese oxide ($LiMn_2O_4$, LMO) cathode. Because the Li^+ ion diffusion in the active material particles must be affected by the spinel structure of LMO, the difference of the heterogeneity from LFP with the olivine structure will promote the further understandings for the cathode reaction mechanism. In this study, the chemical state mappings for the LMO cathode were carried out using the XAFS imaging technique by applying the constant voltages to compare the heterogeneity with those under the constant current conditions.

2. Experimental

An LMO cathode, two separator sheets, and a Li anode were assembled in an Al-laminated battery cell for the XAFS imaging measurement. The cathode was composed of LMO prepared by the solid-state reaction, acetylene black, and polyvinylidene difluoride with the mass ratio of 70:15:15. The imaging XAFS measurements at the Mn K edge were performed at BL-4 of SR Center (Ritsumeikan Univ.) and NW2A of PF-AR (KEK). The discharging process at 3.0 V was measured for 3000 s after the full charge for 12 h. The succeeding charging process at 4.3 V was monitored for further 3000 s.

3. Results and Discussion

Figure 1 shows the change of the acquired chemical state maps during a discharging and charging cycle. The chemical state of LMO was evaluated according to the XANES spectra of standard samples (LMO and λ-MnO_2). The blue pixel indicates that the average oxidation state of Mn at that position corresponds to that in LMO before the charging process. At the fully charged state (Fig. 1A), all Mn species are homogeneous in the cathode plate. It is found that an apparent reaction distribution is not observed in the chemical state map at the transient state of charge during the discharging process, as shown in Fig. 1B. Such a homogeneous chemical state was also observed at the final map (Fig. 1C) and was repeated during the charging process (Fig. 1D-E). As shown in Fig. 1F-G, the homogeneous maps were also observed during the constant current charging and discharging processes. The observed homogeneous chemical state maps of LMO are in marked contrast to those of LFP, in which many reaction spots were appeared in the order of sub mm. The origin of the difference can be assigned to the spinel structure of LMO, for which the multidirectional migration of Li^+ is permitted in the LMO particle. In the case of LFP, the Li^+ ion aligned linearly in the olivine structure.

This study shows that the current time resolution of the 2D XAFS imaging technique is insufficient to observe the chemical state relaxation after the Li^+ insertion/desertion event, and such dynamic measurements will be achieved using the next-generation XAFS imaging technique based on the dispersive X-ray optics.

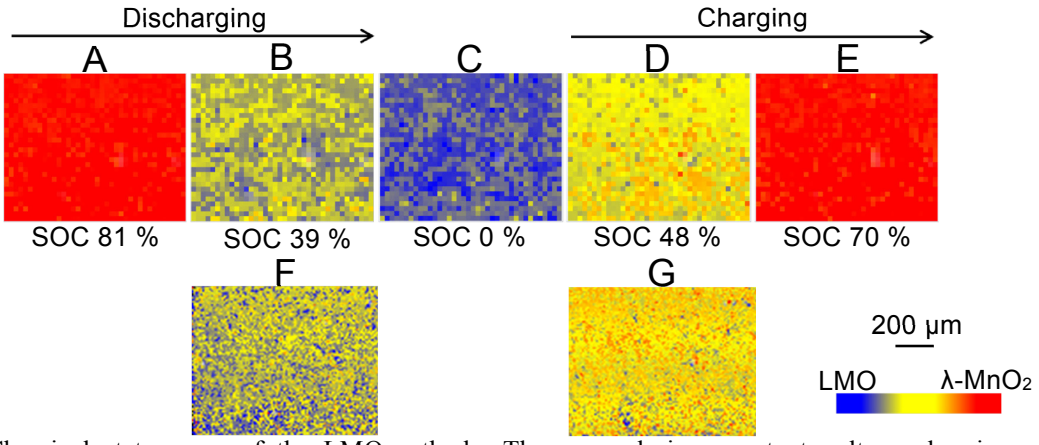

Fig. 1 Chemical state maps of the LMO cathode. The maps during constant voltage charging and discharging processes are shown in A-E, and the maps during constant current charging and discharging processes are shown in F and G, and these SOCs are similar to B and D respectably.

References

[1] M. Katayama, K. Sumiwaka, R. Miyahara, H. Yamashige, H. Arai, Y. Uchimoto, T. Ohta, Y. Inada, and Z. Ogumi, *J. Power Sources*, **269**, 994 (2014).